PHASE TRANSITIONS

Ferroelectricity and Pressure-Induced Phase Transitions in HgTiO₃

A. I. Lebedev

Moscow State University, Moscow, 119899 Russia
e-mail: swan@scon155.phys.msu.ru
Received December 21, 2011

Abstract—Using ab initio density functional theory, the ground state of mercury titanate is determined and phase transitions occurring in it at pressures $P \leq 210$ kbar are analyzed. It is shown that the $R3c$ structure experimentally observed in HgTiO₃ is metastable at $P = 0$. The ground state structure at $T = 0$ varies according to the scheme $R3c \longrightarrow R\bar{3}c \longrightarrow Pbnm$ with increasing pressure in agreement with available experimental data. It is shown that the appearance of ferroelectricity in HgTiO₃ at $P = 0$ is associated with an unstable soft mode. Some properties of crystals in the $R\bar{3}c$ phase are calculated, in particular, the band gap in the GW approximation ($E_g = 2.43$ eV), which is in better agreement with experimental data than the value obtained in the LDA approximation (1.49 eV). An analysis of the thermodynamic stability explains why the synthesis of mercury titanate is possible only at high pressures.

DOI: 10.1134/S1063783412080185

There are only a few studies of mercury titanate HgTiO₃ that indicate its interesting, but contradictory ferroelectric properties. Mercury titanate can be synthesized under a pressure of 60–65 kbar [1, 2]. These crystals have a rhombohedrally distorted perovskite structure. Observation of the second harmonic generation in HgTiO₃ at 300 K [1] enabled one to propose that the space group of the crystal is $R3c$; however, because of a limited accuracy, the atomic coordinates were determined only for the centrosymmetric $R\bar{3}c$ structure. Subsequent studies of dielectric properties of mercury titanate [2, 3] did not detect pronounced dielectric anomalies: a wide strongly asymmetric peak with a maximum near 220 K and with an appreciable hysteresis in the cooling–heating cycle as well as a weak narrow peak near 515 K were observed on the temperature dependence. At 300 K, no dielectric hysteresis loops were appeared up to fields of 10^6 V/m [2, 3]. Scanning calorimetry detected weak anomalies in the 420–480 K temperature range [2, 3]; however, these temperatures differed from the temperatures of peaks in the dielectric constant. Furthermore, X-ray studies under hydrostatic pressure [2, 3] detected non-monotonic behavior of the d_{024} interplanar distance and the (104)–(110) doublet splitting at a pressure of ~20 kbar, which were explained by the rhombohedral-to-cubic phase transition. The electronic structure of the rhombohedral and cubic modifications of HgTiO₃ was studied in [4]; it was shown that the rhombohedral phase is a semiconductor and the cubic phase is a metal.

To resolve the contradictions concerning the ferroelectric properties of HgTiO₃ and to obtain new data on this compound, in this paper, ab initio calculations of physical properties of mercury titanate were performed.

The calculations were carried out within the density functional theory by analogy with the previous study [5]. The pseudopotentials for Ti and O atoms used in the calculations were taken from that study, the scalar–relativistic pseudopotential for the Hg atom was constructed according to the RRKJ scheme [6] using the OPIUM program for the configuration Hg²⁺ ($5d^{10}6s^06p^0$) with the following parameters: $r_s = 1.78$, $r_p = 2.0$, $r_d = 1.78$, $q_s = 7.37$, $q_p = 7.07$, $q_d = 7.37$ a.u. (for the notation of parameters, see [5]). The plane-wave energy cut-off used in the calculations was 30 Ha (816 eV). Integration over the Brillouin zone was performed on the $8 \times 8 \times 8$ Monkhorst–Pack mesh. To test the quality of the mercury pseudopotential, the calculations were carried out for two polymorphs of HgO with orthorhombic and rhombohedral structures. The former one (the montroydite mineral) had a slightly lower total energy. The calculated lattice parameters of these phases ($a = 3.4663$ Å, $b = 6.6253$ Å, $c = 5.3013$ Å, and $a = 3.5092$ Å, $c = 8.5417$ Å, respectively) were in reasonable agreement with experimental data [7] ($a = 3.5215$ Å, $b = 6.6074$ Å, $c = 5.5254$ Å; $a = 3.577$ Å, $c = 8.681$ Å). The phonon spectra were calculated using the scheme similar to that used in [5].

The calculated phonon spectrum of HgTiO₃ with a cubic perovskite structure (space group $Pm3m$) is shown in Fig. 1. One can see that two types of instabil-
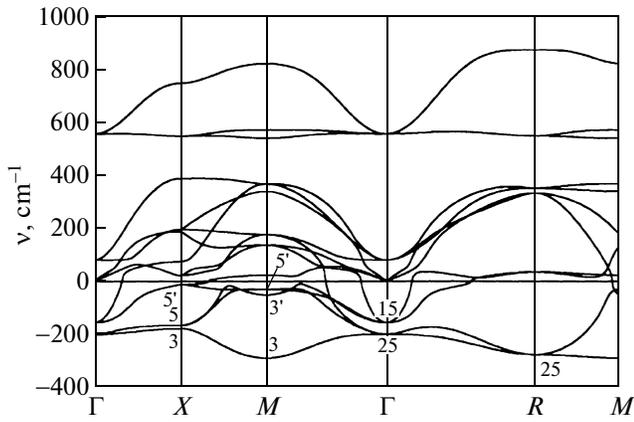
Fig. 1. Phonon spectrum of $HgTiO_3$ in the cubic *Pm3m* phase. Labels near the curves indicate the symmetry of unstable modes. The absence of LO−TO splitting at the Γ point is associated with metallic conductivity of the phase.

ity simultaneously appear in mercury titanate: the stronger one associated with deformation and rotation of octahedra, which is not accompanied with the appearance of dipole moments (the $\Gamma_{25}-X_3-M_3-\Gamma_{25}-R_{25}-M_3$ branch), and the ferroelectric (antiferroelectric at the Brillouin zone boundary) one (the $\Gamma_{15}-X_5'-M_3'-\Gamma_{15}$ branch). The absence of LO−TO mode split-

Table 1. Energy and volume per formula unit in different distorted phases of $HgTiO_3$ at $P = 0$

Unstable mode	Space group	Energy, meV	Cell volume, Å^3
—	$Pm3m$	0	57.573
X_3	$P4_2/mmc$	−88	57.275
Γ_{15}	$R3m$	−94	58.923
Γ_{15}	$R4mm$	−122	59.444
Γ_{25}	$P\bar{4}m2$	−139	57.088
Γ_{15}, Γ_{25}	$Amm2$	−151	59.749
X_5	$Pmma$	−202	57.916
X_5	$Cmcm$	−306	57.867
Γ_{25}	$R32$	−467	56.956
R_{25}	$I4/mcm$	−778	56.188
M_3	$P4/mbm$	−809	56.195
$R_{25} + M_3$	$Pbnm$	−936	**55.853**
R_{25}	$Imma$	−940	56.099
R_{25}	$R\bar{3}c$	−974	56.336
A_{2u}	$R3c$	−982	56.632
—	$R\bar{3}$	**−1059**	60.140

Note: The energy of the cubic phase is taken as the energy reference. The phase with the lowest specific energy and the phase with the lowest specific volume are denoted by bold font.

ting at the Γ point is explained by the metallic character of the band structure of cubic $HgTiO_3$.

To determine the ground state structure, energies of different distorted phases which arise from the cubic perovskite structure during condensation of the above determined unstable modes were calculated taking into account their degeneracy (Table 1). Among these phases, the $R3c$ one has the lowest energy. It is formed from the cubic structure by antiphase rotations of octahedra about all three fourfold axes as a result of condensation of the triply degenerate R_{25} mode at the Brillouin zone boundary (the $a^-a^-a^-$ Glazer tilt system). The energy of this phase is even lower than that of the *Pbnm* phase, in contrast to other titanates of Group II elements [5]. We note that as the structure becomes more distorted, the overlap of the energy bands disappears, and all phases with energies below 300 meV are semiconductors.

The ferroelectric instability of the parent cubic structure of $HgTiO_3$ is also retained in the $R\bar{3}c$ phase. Calculations show that unstable modes of symmetry A_{2u} and E_u with frequencies $135i$ and $21i$ cm^{-1} are observed in the phonon spectrum of this phase at the Γ point. Among the corresponding ferroelectrically distorted phases, the $R3c$ phase has the lowest energy. The fact that this phase corresponds to the ground state is proved by that all phonon frequencies at the Brillouin zone center and at high-symmetry points *A*, *D*, and *Z* at its boundary are positive, and the elastic moduli matrix is positive-definite (see below). The calculated lattice parameters and atomic coordinates in the $R\bar{3}c$ and $R3c$ structures are given in Table 2.

It is seen that they are in good agreement with experimental data [1]. The calculated interatomic distances for the $R\bar{3}c$ phase and average calculated distances for the $R3c$ phase are also in good agreement with interatomic distances obtained from X-ray diffraction studies (Table 3).

In addition to the phases derivative of the cubic perovskite structure, the possible formation of other phases should be considered, in particular, the ilmenite structure characteristic of titanates of Group II elements, i.e., $MgTiO_3$, $ZnTiO_3$, and $CdTiO_3$ [7]. Calculations showed that the ilmenite structure (space group $R\bar{3}$) has the lowest energy at normal pressure ($P = 0$) among the considered phases (Table 1). The fact that the $R\bar{3}c$ or $R3c$ phases are observed in X-ray experiment enables to suppose that these phases are metastable. Their metastability is obviously associated with the significant difference between $R3c$ ($R\bar{3}c$) and $R\bar{3}$ structures in both the lattice parameter and the rhombohedral angle (see Table 2). Therefore, the phase transition between them is the first-order transition for which a wide metastability region is character-

Table 2. Lattice parameters and atomic coordinates in the mercury titanate phases with space groups $R3c$, $R\bar{3}c$, and $R\bar{3}$ at $P = 0$ and the space group $Pbnm$ at 141 kbar

Phase	a, Å	α, deg	Atom	Position	x	y	z
$R3c$	5.4984	58.4093	Hg	2a	0.24904	0.224904	0.24904
			Ti	2a	−0.00333	−0.00333	−0.00333
			O	6b	0.66598	−0.15240	0.25846
$R\bar{3}c$	5.4881	58.4252	Hg	2a	0.25000	0.25000	0.25000
			Ti	2b	0.00000	0.00000	0.00000
			O	6e	0.65983	−0.15983	0.25000
$R\bar{3}c$ (exp.)* [1]	5.4959	58.59	Hg	2a	0.25	0.25	0.25
			Ti	2b	0.0	0.0	0.0
			O	6e	0.665	−0.165	0.25
$R\bar{3}$	5.8304	53.9320	Hg	2c	0.36869	0.36869	0.36869
			Ti	2c	0.84974	0.84974	0.84974
			O	6f	0.55966	−0.03220	0.19275
$Pbnm$	5.2678(a)	–	Hg	4c	−0.00445	0.03190	0.25000
	5.2983(b)		Ti	4b	0.50000	0.00000	0.00000
	7.5501(c)		O	4c	0.08502	0.47264	0.25000
			O	4d	0.69594	0.30216	0.04431

* Coordinates were recalculated for the rhombohedral setting.

istic. The fact that namely the metastable $R3c$ ($R\bar{3}c$) phase appears during the synthesis can be caused by that HgTiO$_3$ is synthesized at a pressure of 60−65 kbar at which (as shown below) the $R\bar{3}c$ phase is the most stable. The energy of two more possible hexagonal HgTiO$_3$ phases with the two-layer BaNiO$_3$ structure and the six-layer hexagonal BaTiO$_3$ structure (the space group of both is $P6_3/mmc$) is higher than the energy of the $Pm3m$ phase by 269 and 73 meV, respectively.

We discuss now the ferroelectric properties and the nature of the ferroelectric phase transition in HgTiO$_3$. Since the change in the Hg−O bond lengths during phase transition to the ferroelectric phase does not exceed 0.1 Å, and the energy difference of the $R3c$ and $R\bar{3}c$ phases is only 8.1 meV, it is unlikely that the Curie temperature in HgTiO$_3$ will exceed 300 K. Therefore, it is in better agreement with a temperature of 220 K at which the dielectric constant maximum was experimentally observed. The absence of the dielectric hysteresis loops at 300 K also supports this interpretation. Therefore, in what follows, being oriented on experiments performed at 300 K, we will focus on the properties of the $R\bar{3}c$ phase. The fact that the authors of [1] observed a signal of the second harmonic at room temperature can be associated with the sample defectness which is discussed in what follows.

An analysis of the eigenvector of the A_{2u} ferroelectric mode in the $R\bar{3}c$ phase shows that the displacements of Hg atoms in this mode is smaller than that of Ti atoms by a factor of 22. This means that collective displacements of the titanium atoms with respect to the oxygen ones are responsible for the ferroelectric phase transition, rather than the mercury atom jumps between wells of the two-well potential. The effective Born charges of the mercury atoms also indicate their weak ferroelectric activity: they are $Z_{xx}^* = Z_{yy}^* = 3.20$ and $Z_{zz}^* = 2.42$ and differ slightly from the nominal ionic charge.

The calculated static dielectric constant at 0 K in the $R3c$ phase is almost isotropic ($\varepsilon_{xx} = 97$, $\varepsilon_{zz} = 101$);

Table 3. Interatomic distances in the HgTiO$_3$ phases with space groups $R3c$ and $R\bar{3}c$

Atom pair	Distance, Å			Number of bonds
	this work		Ref. [1]	
	$R3c$	$R\bar{3}c$		
Hg−O	2.198	2.195	2.20(4)	3
Hg−O	2.698, 2.888	2.786	2.77(4)	3 + 3
Hg−O	3.172	3.162	–	3
Ti−O	1.906, 2.064	1.977	1.96(4)	3 + 3

Table 4. Calculated frequencies of optical phonons at the Γ point of the Brillouin zone for HgTiO$_3$ with $R3c$, $R\bar{3}$, and $Pbnm$ structures (the latter is at $P = 147$ kbar)

Structure $R3c$				Structure $Pbnm$					
mode	v, cm^{-1}	mode	v, cm^{-1}	mode	v, cm^{-1}	mode	v, cm^{-1}	mode	v, cm^{-1}
A_1	78	E	81	A_g	68	B_{1g}	439	B_{1u}	530
	181		121		113		502	B_{2u}	38
	379		139		144		782		86
	476		165		277	B_{2g}	104		141
A_2	62		274		417		266		190
	347		312		462		450		345
	355		443		559		542		356
	417		495	A_u	65		819		431
	753		515		74	B_{3g}	118		496

Structure $R\bar{3}$									
A_g	73	E_g	94		108		226		524
	204		189		141		353	B_{3u}	58
	306		311		303		539		114
	440		442		375		732		165
A_u	651	E_u	565		498	B_{1u}	38		246
	133		148		539		84		301
	348		256	B_{1g}	80		134		380
	477		371		103		243		403
	647		452		139		387		448
					350		475		547

in the $R\bar{3}$ phase, the dielectric constant is notably lower ($\varepsilon_{xx} = 28$, $\varepsilon_{zz} = 27$). For comparison, the maximum dielectric constant experimentally observed at 220 K is ~800 [2, 3]. The calculated spontaneous polarization in the $R3c$ phase appears unexpectedly high, $P_s = 0.37$ C/m^2. This is probably a result of the large effective charge of the A_{2u} mode in the paraelectric phase ($Z_{\mathrm{eff}}^* = 12.66$).

We consider now some other physical properties of HgTiO$_3$ at $P = 0$. The calculations of the electronic structure performed in this work confirmed the data of [4] that the $R\bar{3}c$ phase is a direct-gap semiconductor with the band extrema located at the Γ point. The band gap of mercury titanate at $P = 0$ is $E_g^{\mathrm{LDA}} = 1.49$ eV, its pressure coefficient is $dE_g^{\mathrm{LDA}}/dP = +0.44$ meV/kbar. The value of E_g obtained in the LDA approximation agrees with the value of 1.6 eV found in the GGA approximation using the FP-LAPW method [4]. However, both results disagree with the experimental fact that HgTiO$_3$ crystals are light yellow [1]. It is well known that the density functional theory always underestimates the band gap because of its limitations with respect to the calculation of the excited states energy. One of the approaches that yield the E_g values

in good agreement with experiment is based on the consideration of many-body effects (electron correlations, dynamic screening, local field effects) within the GW approximation [8]. The calculations performed in this work within this approximation yielded $E_g^{GW} = 2.43$ eV in the $R\bar{3}c$ phase, which agrees much better with the sample color reported in [1] than the band gap in the LDA approximation.

The elastic moduli tensor in the $R\bar{3}c$ phase is presented by seven independent components: $C_{11} = C_{22} = 348.0$ GPa, $C_{33} = 260.3$ GPa, $C_{12} = 178.5$ GPa, $C_{13} = C_{23} = 149.9$ GPa, $C_{44} = C_{55} = 76.3$ GPa, $C_{66} = 84.8$ GPa, and $C_{14} = -C_{24} = C_{56} = 18.3$ GPa. The bulk elastic modulus calculated from them is $B = 205.8$ GPa; it slightly differs from the value of 178 GPa obtained in [4] ignoring the relaxation of internal degrees of freedom.

To interpret future experiments on infrared (IR) reflection and Raman scattering, the phonon frequencies calculated at the Γ point for $R3c$, $R\bar{3}$ phases at normal pressure and the $Pbnm$ phase at 147 kbar, given in Table 4, can be useful. In the low-temperature $R3c$ phase, the A_1 and E modes are active in both IR and Raman spectra. In the $R\bar{3}$ phase, the A_u and E_u modes

are IR active; the A_g and E_g modes are Raman active. In the high-pressure *Pbnm* phase, the B_{1u}, B_{2u}, and B_{3u} modes are IR-active; the A_g, B_{1g}, B_{2g}, and B_{3g} modes are active in Raman spectra.

To discuss the experimental data [2, 3] on the effect of the hydrostatic pressure on the $HgTiO_3$ structure, we calculated the properties of mercury titanate under pressure. At a nonzero pressure, the phase which is characterized by the lowest enthalpy $H = E_{tot} + PV$, rather than by the lowest total energy E_{tot}, is thermodynamically stable at $T = 0$. To compare phases with different number of molecules in the unit cell, we use the specific total energy and the specific unit cell volume defined per one formula unit. Calculations show that as the pressure changes, the relative contribution of the PV term to the change in H is ~95% in the crystals under study. Therefore, the phases with the lowest specific volume should become the most stable as the pressure increases. As follows from Table 1, the *Pbnm* phase has the smallest volume at $P = 0$ among the considered phases; then, in order of increasing the specific volume, the phases are arranged as follows: *Imma*, *I4/mcm*, *P4/mbm*, $R\bar{3}c$, *R3c*. The largest unit cell volume is characteristic of the ilmenite $R\bar{3}$ phase, whose total energy at $P = 0$ is the lowest. This enables to expect that the sequence of stable phases will vary with increasing pressure as follows: $R\bar{3} \longrightarrow R3c \longrightarrow Pbnm$. In addition, the suppression of ferroelectricity (the $R3c \longrightarrow R\bar{3}c$ phase transition) should be observed with increasing pressure.

The differences between enthalpies of the phases under consideration and the enthalpy of the $R\bar{3}c$ phase as a function of pressure are shown in Fig. 2. It is seen that the $R\bar{3} \longrightarrow R3c$ and the $R\bar{3}c \longrightarrow Pbnm$ phase transitions occur in $HgTiO_3$ at $P = 38$ and 141 kbar, respectively. Since the specific volume of the unit cell changes stepwise (by 6 and 0.71%, respectively) at both phase transitions, they should be of the first order. The *Imma* phase, whose enthalpy at $P = 0$ is lower than that of the *Pbnm* phase, becomes energetically less favorable with increasing pressure, and can be excluded from the consideration. The similar behavior, when the stable $R\bar{3}$ phase transformed to the pressure-stabilized *Pbnm* phase under high temperatures and pressures and then relaxed from the latter phase to the metastable $R\bar{3}c$ phase as pressure was released, was also observed in $MnTiO_3$ [9], $FeTiO_3$ [10], and $ZnGeO_3$ [11]. Ferroelectric $LiTaO_3$ also exhibits the $R3c \longrightarrow Pbnm$ phase transition at high pressures [12].

The present calculations enable to propose a new interpretation of the phase transition observed in X-ray experiments at hydrostatic pressure [2, 3]. The energy of the cubic *Pm3m* phase, which was attributed to the high-pressure phase in [2, 3], is higher than that
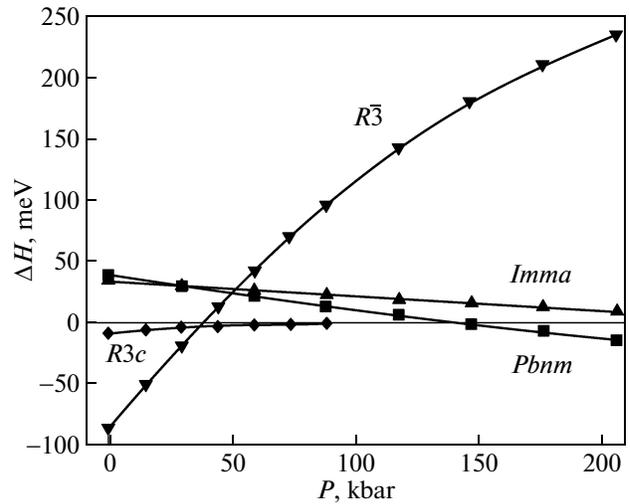
Fig. 2. Difference between the enthalpies of different phases and the enthalpy of the $R\bar{3}c$ phase in $HgTiO_3$ as a function of hydrostatic pressure.

of the $R\bar{3}c$ phase by almost 1 eV, and the specific cell volume of this phase exceeds that of the $R\bar{3}c$ phase (Table 1). This means that the sufficiently large difference between the enthalpies of these phases will only increase with increasing pressure. Therefore, the *Pm3m* phase cannot be considered as a high-pressure phase. According to our calculations, the rhombohedron angle in the $R\bar{3}c$ phase increases with a rate of 0.0054°/kbar with increasing pressure; therefore, at $P = 20$ kbar the structure should remain strongly distorted, and the relative decrease in the interplane distance should be $P/3B \approx 0.32\%$, which is several times smaller than that observed at the phase transition. However, if we admit that the pressures in [2, 3] were determined with an error (according to our estimates, they are underestimated by a factor of 5–7) and take the relative change in the interplane distance d_{024}[1] as a measure of pressure, the agreement between the present calculations and the experimental data becomes satisfactory. For example, at the $R\bar{3}c \longrightarrow Pbnm$ transition point (141 kbar), the calculated decrease in the d_{024} interplane distance in comparison with the case of $P = 0$ is 2.0%, whereas the experimental value is 2.3%, and the calculated jump of the average interplane distance[2] at the phase transition point (0.054%) is close to the experimental value of ~0.05%.

---

[1] The d_{024} value at $P = 0$, shown in Fig. 3 of [2], does not correspond to the lattice parameters given in the paper for this pressure (disagreement is ~5%).

[2] During the $R\bar{3}c \longrightarrow Pbnm$ phase transition, the peak (012) splits into two components with indices (110) and (002).
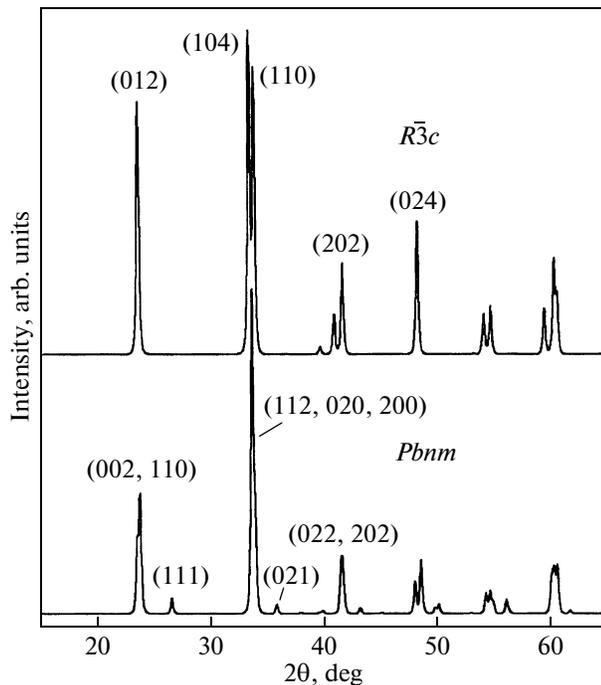
Fig. 3. Calculated X-ray diffraction patterns of $R\bar{3}c$ and *Pbnm* phases of mercury titanate at $P = 141$ kbar (for CuK_α radiation).

The lattice parameters and atomic coordinates in the *Pbnm* structure at 141 kbar are given in Table 2.

The calculated X-ray diffraction patterns of $R\bar{3}c$ and *Pbnm* phases at 141 kbar are shown in Fig. 3. The calculated X-ray diffraction pattern of the *Pbnm* phase is indeed similar to the experimental X-ray diffraction pattern of the high-pressure phase [2, 3]. During the transition to the orthorhombic phase, the (012) line broadens, since a pair of closely spaced reflections (002) and (110) appears in the orthorhombic phase. The new line (021) appearing in the orthorhombic phase is easily seen in the X-ray diffraction patterns recorded as the pressure is released. A notable disagreement between the experimental and calculated X-ray diffraction patterns is the absence of the (111) line in the X-ray diffraction pattern of the high-pressure phase. It is possible that this disagreement results from an incompleteness of the structural transformation. Therefore, to confirm the interpretation proposed in this paper, additional studies of HgTiO$_3$ under pressure are required.

As noted above, the contradiction between the absence of dielectric hysteresis loops in HgTiO$_3$ at 300 K and the observation of the second harmonic

generation signal can be caused by the existence of defects. Indeed, according to the data of [1], the samples rapidly darkened upon exposure to light. The absence of a sharp peak in the dielectric constant can also be caused by defects. This propensity of HgTiO$_3$ for the defect formation is confirmed by simple ab initio calculations of its thermodynamics: at $P = 0$, the enthalpy of the $R\bar{3}c$ phase of mercury titanate is higher than the sum of enthalpies of orthorhombic HgO and rutile TiO$_2$ by 150 meV (per formula unit). This means that mercury titanate is thermodynamically unstable with respect to its decomposition into starting components. However, since the specific volume of the HgTiO$_3$ unit cell is noticeably smaller than the sum of specific volumes of HgO and TiO$_2$, the stability of HgTiO$_3$ increases with increasing pressure. For example, at a pressure of 58.8 kbar, the HgTiO$_3$ enthalpy appears lower than the sum of enthalpies of orthorhombic HgO and rutile TiO$_2$ by 75 meV. This explains why the synthesis of mercury titanate is possible only under high-pressure conditions.

The calculations presented in this paper were performed on the laboratory computer cluster (16 cores).

REFERENCES

1. A. W. Sleight and C. T. Prewitt, J. Solid State Chem. **6**, 509 (1973).
2. Y. J. Shan, Y. Inaguma, T. Nakamura, and L. J. Gauckler, Ferroelectrics **326**, 117 (2005).
3. Y. J. Shan, Y. Inaguma, H. Tetsuka, T. Nakamura, and L. J. Gauckler, Ferroelectrics **337**, 71 (2006).
4. H. S. Nabi, R. Pentcheva, and R. Ranjan, J. Phys.: Condens. Matter **22**, 045504 (2010).
5. A. I. Lebedev, Phys. Solid State **51** (2), 362 (2009).
6. A. M. Rappe, K. M. Rabe, E. Kaxiras, and L. D. Joannopoulos, Phys. Rev. B: Condens. Matter **41**, 1227 (1990).
7. *Springer Materials: The Landolt-Börnstein Database*; URL http://www.springermaterials.com/navigator/.
8. G. Onida, L. Reining, and A. Rubio, Rev. Mod. Phys. **74**, 601 (2002).
9. N. L. Ross, J. Ko, and C. T. Prewitt, Phys. Chem. Miner. **16**, 621 (1989).
10. K. Leinenweber, W. Utsumi, Y. Tsuchida, T. Yagi, and K. Kurita, Phys. Chem. Miner. **18**, 244 (1991).
11. H. Yusa, M. Akaogi, N. Sata, H. Kojitani, R. Yamamoto, and Y. Ohishi, Phys. Chem. Miner. **33**, 217 (2006).
12. J. Li, X. Zhou, W. Zhu, J. Li, and F. Jing, J. Appl. Phys. **102**, 083503 (2007).

Translated by A. Kazantsev